

EFFECT OF SURFACE TREATMENT ON ARRAY MICROPHONE SELF-NOISE

Stephen M. Jaeger*

Aerospace Computing, Inc.
Los Altos, California
USA

W. Clifton Horne† and Christopher S. Allen*

NASA Ames Research Center
Moffett Field, California
USA**ABSTRACT**

A method for reducing the flow-induced self-noise of acoustic array microphones was demonstrated in a wind tunnel. Unsteady boundary-layer flow in the wind tunnel induces large pressure fluctuations on exposed, flush-mounted microphone diaphragms, reducing the signal-to-noise capability of microphone arrays. Two important steps were taken to reduce this background noise. First, the microphones were recessed to separate the microphones from the unsteady flow. Second, a porous surface material was placed above the microphones to act as an aerodynamic surface while allowing acoustic signals to pass through to the microphones. Previous attempts at this approach used perforated plates as the surface material, which tended to fatigue in the unsteady flow. The increased acoustic impedance of thicker materials caused reverberation between the surface and the microphone mounting plate. This latest attempt used a stretched sheet of Kevlar® as the surface. The extreme strength and durability of the Kevlar® withstood flow-induced fatigue while providing very low acoustic impedance with little attenuation of sound for most frequencies. Data is presented for two wind tunnel tests that demonstrate the capabilities of the recessed Kevlar® array.

NOMENCLATURE

B	Number of data blocks
C_p	Coefficient of pressure
d	Convective disturbance wavelength (mm)
e'	Transpose of array steering vector
f	Frequency (Hz)
F_m	Total signal sampled at microphone m (Pa)
F	Vector of sampled microphone signals (Pa)
K	Maximum amplitude of pressure disturbance (Pa)
L_p	Sound Pressure Level (dB)
M	Number of microphones in array

* Aeroacoustics Engineer, Senior Member, AIAA.

† Aeroacoustics Engineer, Associate Fellow, AIAA

M_∞	Free-stream Mach number
N	Vector of noise sampled at microphones (Pa)
p'_{BL}	Boundary-layer pressure disturbance (Pa)
S	Vector of sampled source contributions (Pa)
SNR_m	Signal-to-noise ratio at microphone
U_C	Convection (free-stream) velocity (m/s)
x	Distance along wall (mm)
y	Distance from wall (mm)
α	Spatial angular frequency (radians/sec)
Δf	Narrow band frequency resolution (Hz)
$\delta_{95\%}$	95% confidence in peak level (dB)
ϵ	Sinusoidal displacement amplitude (mm)

INTRODUCTION

The advent of modern computer processing and electronics has made phased array processing practical for numerous applications including full-scale fly-over measurements¹ and wind tunnel studies of aerospace noise sources. Phased arrays have all but replaced earlier methods for locating noise sources such as dual sideline correlation², acoustic mirrors^{3,4} and sound intensity⁵. Whether processing is done in the time domain^{6,7} or the frequency domain^{8,9}, the combined contributions of multiple microphones enable researchers to distinguish and quantify noise sources in a manner not possible with individual microphones. Further, the phased microphone array's ability to discriminate against background noise makes it particularly useful for airframe noise studies, as the noise sources are usually quieter than the prevalent wind tunnel background noise.

Self-Noise Reduction Techniques

Microphone array measurements have been used to quantify jet and airframe noise sources in closed¹⁰⁻¹² and open^{13,14} wind tunnel test sections with much success. Although in-flow wind tunnel array measurements are not burdened by the need to apply shear layer corrections to

multiple source paths, the background noise level at the microphones is high because of the turbulent boundary layer flowing over the exposed microphone diaphragms. The influence of this noise can be reduced by increasing the number of microphones, but cost and size constraints limit the practical number. Increasing the acquisition time can also reduce the influence of random, uncorrelated background noise^{15,16}, but limited computer resources and the expense of wind tunnel testing puts a bound on available run time.

Another method, often used during single microphone acquisitions, is to subtract out the tunnel-empty background noise¹³. While straightforward in theory, the task of evaluating the tunnel empty-noise in a consistent manner often requires multiple test runs to achieve an accurate statistical set¹⁷. Processing techniques, such as replacing the covariance matrix diagonal with zeroes or an averaged spectra, may also reduce the influence of flow noise, but this method is limited somewhat by the necessity for completely incoherent self noise at each microphone^{13,16}.

Previous Attempts at Separating Array Microphones and Flow

Previous studies have validated the approach of covering and recessing flush-mounted microphones to alleviate flow noise^{12,16,18-20}. If the actual background noise can be reduced, less data and fewer time averages are required to resolve potential sources. Compared to the expense of doubling the number of microphones or the acquisition time to achieve a 3 dB increase in dynamic range, even a modest surface treatment would be well worth the investment.

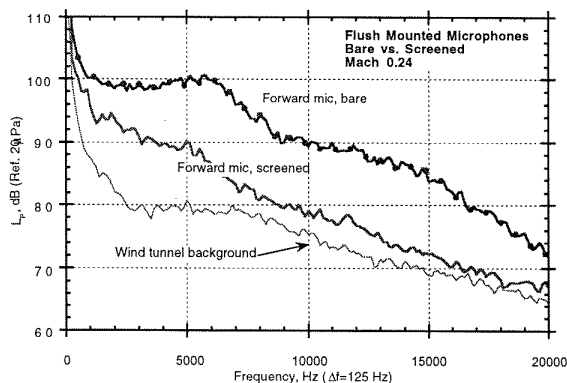


Figure 1. Self-noise of plate-mounted array microphones. Individual screens reduced the self-noise by up to 20 dB. (The ambient wind tunnel background noise was measured with a single in-flow microphone.)

Plate-mounted microphone arrays have been utilized at Ames since 1993¹⁰. The first attempt at controlling the flow noise over the flush-mounted microphones was demonstrated in 1994 during a wind tunnel test of a jet engine nozzle. Each microphone of a 16-element Mill's Cross¹⁰ was installed behind nylon and fine metal screens. The physical separation of microphone and flow was

provided by the gap between the factory-built grid and the diaphragm. The results in Figure 1 show a reduction of up to 20 dB for some of the forward, screened microphones as compare to bare microphones. The background noise reduction was not as prominent for the rear microphones. Also shown, for comparison, is the empty wind tunnel background noise as measured by a single in-flow microphone with an aerodynamic forebody.

At the same time, a research program conducted in the NASA Ames 7-by 10-Foot Wind Tunnel (7x10) established a direct correlation between the separation distance and the level of background noise. The microphones were recessed from the wind tunnel's turbulent boundary layer by a porous surface. Although several surface treatments were used, including fine mesh screens and porous plates, acoustic reverberation between the screen and the array surface limited its usefulness as a method for reducing flow-induced background noise. Another problem that appeared was "oil-canning" whereby the stiff metal plate would shake and eventually fatigue under the influence of the turbulent boundary layer. Subsequent tests in 1995, using a 40-element array¹¹, sought to eliminate the reverberation and prevent "oil canning" by shouldering the spiral array arms with foam inserts as shown in Figure 2. This treatment, however, had a significant effect on the array's directionality at shallow grazing angles.

These previous studies suggested that the ideal array surface treatment requires a thin, light, porous surface with low acoustic impedance that is also strong enough to act as an aerodynamic surface to separate unsteady flow from the bare microphone diaphragms. In response to this, a design study and test program was initiated to develop a suitable surface treatment.

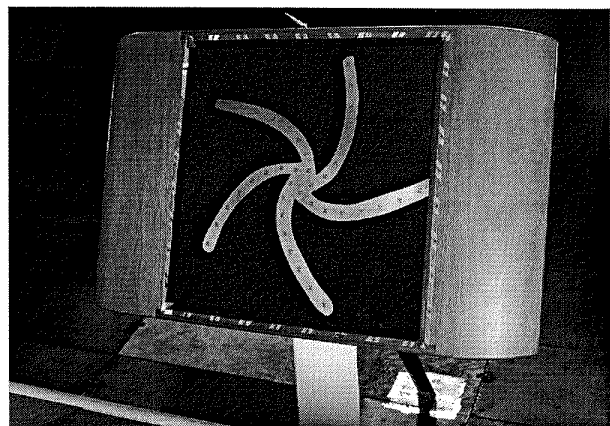


Figure 2. Plate-mounted 40-microphone array. Spiral arms are shouldered within foam inserts. (The surface screen was removed for the photo.)

THEORETICAL DEVELOPMENT

Effect of Self-Noise on Array Measurements

The importance of reducing the self-noise on each microphone can be demonstrated by looking at the influence of noise on the array measurement. The signal

received at a given array microphone, F_m , is taken as the sum of the actual radiated signal received at the microphone, S_m , and the statistically-independent noise measured at the microphone, N_m :

$$F_m = S_m + N_m \quad (1)$$

where the signal, S is assumed to be that derived, via planar processing, from a single, isolated source such that all $|S_i| = |S_M| = |S|$. The noise, N_m , measured at each microphone, is assumed to have equal standard deviation, $\sigma(|N|)$.

The peak array response will occur when the scan location is coincident with the source and the calibrated phase of the steering vector, e' and the source are matched. This relationship is expressed as the dot product, $e' \cdot F$, where F is the vector of sampled microphone signals. From reference 16,

$$\frac{\sigma(|e' \cdot F|_{peak})}{|e' \cdot S|_{peak}} = \frac{1}{\sqrt{M \cdot B}} \frac{\sigma(|N|)}{|S|} \quad (2)$$

That is, the standard deviation of the received signal is directly related to the standard deviation of the noise and inversely related to the square root of the number of microphones, M and data averages, B used in the processing.

The 95% confidence level in the measured array peak dB level, corresponding to 1.96σ , can be expressed as:¹⁶

$$\begin{aligned} \delta_{95\%} &= 1.96\sigma \left(20 \log_{10} |e' \cdot F|_{peak} \right) \\ &\approx \frac{17.05}{\sqrt{M \cdot B}} \frac{\sigma(|N|)}{|S|} \end{aligned} \quad (3)$$

Rearranging Equation (3) by defining the signal-to-noise ratio of a single array microphone, as defined in reference 16:

$$\begin{aligned} SNR_m &= 20 \log_{10} \left(\frac{|S|}{\sigma(|N|)} \right) \\ &= 24.8 - 20 \log_{10}(\delta_{95\%}) - 10 \log_{10}(M) - 10 \log_{10}(B) \end{aligned} \quad (4)$$

Equation (4) can be used to determine the necessary SNR of a microphone array measurement to achieve a 95% confidence level in the peak array level.

Influence of Microphone Recessing

The turbulent flow over the array surface imparts an evanescent pressure wave that decays exponentially over the space between the flow surface and the microphone. One way to analyze the influence of these propagating disturbances is to simulate them as the pressure field in a subsonic, uniform flow over a wavy wall²¹. The pressure fluctuations would then be expressed as:

$$C_p = \left(\frac{2\varepsilon\alpha}{\sqrt{1-M_\infty^2}} \right) \left(e^{-y\alpha\sqrt{1-M_\infty^2}} \right) \sin(\alpha x) \quad (5)$$

Where x is the displacement along the wall and y is the displacement away from the wall. The wavy wall displacement is described by:

$$y_w = -\varepsilon \sin(\alpha x) \quad (6)$$

Where ε is the wall displacement amplitude. By estimating the convective disturbance wavelength to be $d = U_c/f$, where U_c is the convection speed, the spatial angular frequency becomes:

$$\alpha = \frac{2\pi f}{U_c} = \frac{2\pi}{d} \quad (7)$$

Substituting Equations (6) and (7) into Equation (5) as in reference 16, gives,

$$C_p = \left(\frac{4\pi\varepsilon}{d\sqrt{1-M_\infty^2}} \right) \left(e^{-\frac{2\pi y}{d}\sqrt{1-M_\infty^2}} \right) \sin\left(\frac{2\pi x}{d}\right) \quad (8)$$

For $M_\infty \ll 1$ the unsteady, boundary layer pressure disturbance, p'_{BL} becomes:

$$|p'_{BL}| = Kfe \frac{2\pi y}{U_c} \quad (9)$$

and decays as:

$$20 \log_{10}(\Delta p'_{BL}) = -4.3 \frac{4\pi fy}{U_c} \quad (10)$$

Equation (10) was applied to the recessed array design in this paper. For a recess of $y = 12.7$ mm (0.5 in), flow velocity of $U_c = 74.7$ m/s (245 ft/s) and frequency of $f = 3400$ Hz, the decay would be 31.2 dB. This theoretical decay is graphed in Figure 3 for three possible recess distances. The signals will decay faster with frequency as the microphones are separated from the turbulent boundary layer. This is for an ideal situation, as the boundary layer thickness will cause the actual decay to be less. Further, the decay should appear to increase with frequency, but this effect is overtaken at higher frequencies by the scrubbing noise radiated from the interaction of the turbulence with the screen. A smooth screen surface is also important in the design of recessed arrays.

ARRAY DESIGN AND HARDWARE

“Drumhead” Surface Support Design

It was anticipated that a surface with adequate rigidity could be obtained by stretching a pliable, low mass, low impedance material above the recessed microphones. No solid structural support (i.e.: ribs, foam, gratings or pylons) would be necessary to support the material thereby minimizing path interference at shallow look angles. A circular fiberglass ring, similar to a drumhead rim, was designed and fabricated to hold the material in place over the array surface. A 106.7 cm (42.0 in) diameter fiberglass annulus held the material taut by tensioning it over the fiberglass rim. The design allowed for a 12.7 mm (0.5 in) recess over the bare microphones as shown in Figure 4.

The design was constrained by the inside dimensions of an existing aerodynamic array box that will utilize the recessed array for a planned airframe noise test in the NASA Ames 40- by 80-Foot Wind Tunnel. The 12.7 mm (0.5 in) recess was the maximum allowed by the existing dimensions, although a greater recess would be expected to provide even better isolation from turbulent boundary layer noise. A piece of fiberboard was cut to fit outside the circular rim to provide a smooth aerodynamic transition from the wind tunnel wall to the porous surface.

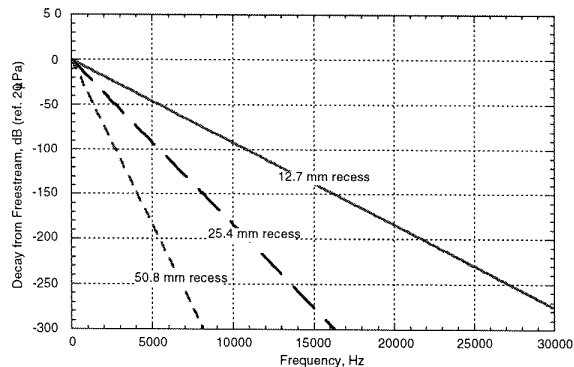


Figure 3. Theoretical decay of pressure wave into recess based on wavy wall analogy.

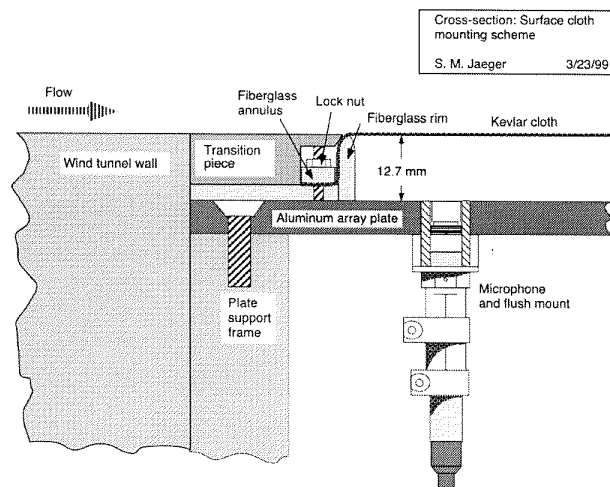


Figure 4. Cross-sectional view of recessed array design.

Array Pattern Design

Design constraints for the above-mentioned test limited the recessed array to 70 6.3 mm (0.25 in) microphones within a 101.2-cm (40.0 in) diameter. The microphones were arranged in five radial lobes as shown in Figure 5. This arrangement allowed the array to fit within the circular drumhead rim and facilitated the interpretation of source shapes during data reduction. The design frequency range was 200 to 25000 Hz. The holes for the microphone array were drilled into a 6.3 mm (0.25 in) thick sheet of 6026

aluminum. All microphones were mounted flush with the plate surface to within 0.13 mm (0.005 in) using custom-built microphone fittings.

The microphone positions were optimized for narrow beam size and minimal sidelobe interference²² using a MATLAB-based simulated annealing code.²³ The annealing technique is a Monte Carlo²⁴ method that distributes the microphones about the array surface according to a user-defined function. In the actual annealing of a steel alloy, atoms move about in the original hot solution from initial, local energy states. The movement of these atoms slows as the steel is carefully cooled. The intent is to allow the atoms to distribute in such a manner as to eliminate weak spots and defects. The intent of simulated array annealing is to randomly move the microphones in response to a simulated energy function. As the “temperature” decreases logarithmically, the allowable movement of the microphones is slowly constrained. At each iterative step, the array pattern is tested for narrow beamwidth and low sidelobes. The process stops when the desirable characteristics are achieved. Although identical constraints can be applied, each simulation will produce a unique array pattern that will satisfy the desired characteristics.

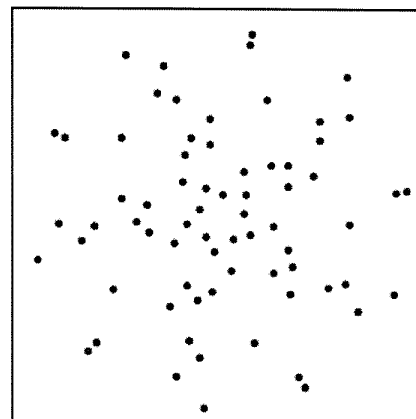


Figure 5. The 5-lobed, 70-element array pattern was generated using simulated annealing.

Hardware and Data Acquisition

All 70 microphones were G. Rasmussen’s TMS model 140BF, quarter-inch free-field microphones. The microphones were connected to 35 TMS model 112AA, 2-channel, DC-powered, adjustable-gain power modules. The signals were acquired by Hewlett-Packard model E1433A high-speed A/D cards on a HP VXI chassis, controlled by an HP 745i computer via a MXI/EISA interface. Although the 16-bit cards are capable of 96 dB in dynamic range, overhead requirements constrained this range to about 84 dB. The 70 microphone signals were sampled at 76800 samples per second, in five separate blocks of 0.53 seconds each, for a total of 2.66 seconds per acquisition. With 70 microphones, each data record represented over 14 million samples. The acquired time domain data was stored in binary format on an Andataco 25-Gbyte GigaRAID storage unit. The binary data was then converted into NetCDF²⁵ format for permanent storage and retrieval.

Processing of the time data was performed using MAPPs, an array processing software package developed at NASA Ames.²⁶ The data were parallel-processed on a dual-processor SGI Octane computer. Classical, frequency-domain, phased array beamforming²⁷ was used for all the cases discussed in this paper. In addition, the diagonal elements were replaced with an average of the off-diagonal elements of the cross-spectral matrix. A correction was also applied to the data to account for convection. The frequency resolution for most of data in this paper was 150 Hz. The best results were obtained with FFT processing of 512 blocks for 400 averages over the 2.66-second data sample.

Spatial integration methods were used to assess the overall level of sources in the image plane of the array. An automatic integration boxing routine locates and boxes significant sources within the scan region. The integration regions were drawn about the sources at the 8 dB down point, typically.

WIND TUNNEL TESTS

CMT Test

The CMT test was a study of a Continuous Moldline Technology (CMT)^{28,29} wing, shown in Figure 6. CMT, in practice, would likely be a flexible membrane spanning the flap/airfoil edge interface. In this test, a solid piece was used for each fixed flap angle of $+35^\circ$ and -40° . The test investigated the airframe noise reduction possibilities of the CMT concept, as compared to that of a simple, hinged flap, installed on the 1.52-meter (60.0 inches) span airfoil. It was suggested that the elimination of the flap edge had the potential to significantly lower the measured airframe noise level to below the noise floor of a typical microphone array. The inability to precisely measure the sound levels of the CMT concept was a concern for the program. Although a 100-element flush surface array was proposed as the principal acoustic measurement system, the 70-element, treated, recessed array was installed during the test in an attempt to lower the array background noise.

Array Concepts Test

Immediately following the CMT study, the Array Concepts test was conducted to investigate coherence and directionality issues associated with phased arrays³⁰. The 70-element recessed array was used exclusively for this test. The array's ability to measure extended noise sources was assessed using the In-Flow Multi-element Acoustic Source (IMAS), shown in Figure 7. The IMAS is a 2.1 meter (84.0 inch) long, aerodynamically-faired, speaker box fitted with five low frequency woofers and five high frequency horns to provide a set of coherent or incoherent noise sources.

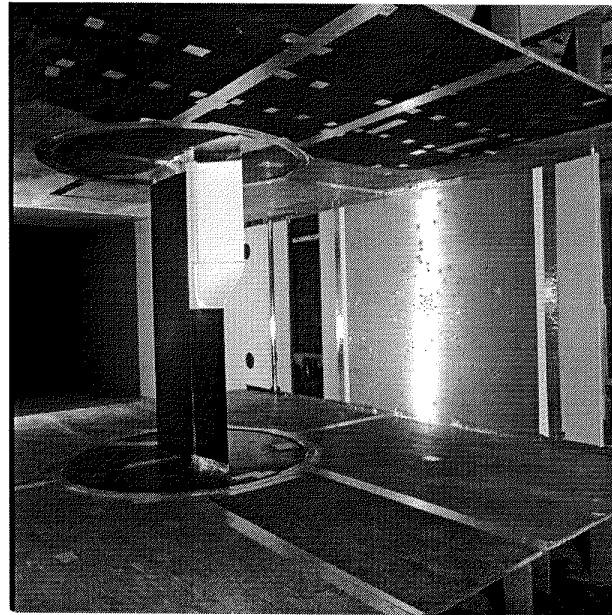


Figure 6. CMT flap mounted in the 7x10 Wind Tunnel with the flush-mounted 100-element array on the far wall.

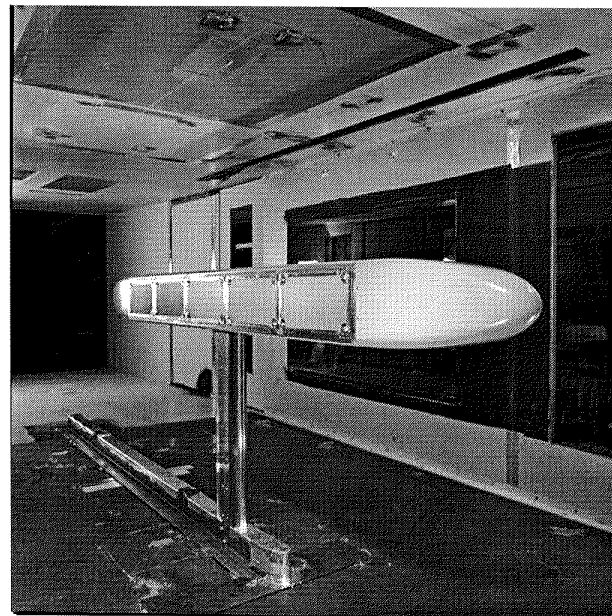


Figure 7. The In-flow Multi-element Acoustic Source (IMAS) provided a controlled set of coherent or incoherent noise sources, as required by the test.

RESULTS AND DISCUSSION

Application of Kevlar

Three surface materials were eventually tested with the array. A sheet of Technetics FM-125 fiberglass cloth was chosen as the first test material because of its low acoustic impedance and low weight. Unfortunately, the fiberglass cloth disintegrated almost immediately in the flow because of its poor resistance to shear forces. Better results were obtained using a sheet of 100 MKS Rayl stainless steel screen, however the stiff material also fatigued under the unsteady loads at the down-stream edge of the array.

Fortunately for the test program, excellent results were obtained using Kevlar[®] cloth as the surface material. Kevlar[®], with a tensile strength of 2700 MN/m² (400 ksi)³¹, is used to repair surfboards and to provide penetration resistance for bullet-proof vests. It is very resistant to shear load yet has low acoustic impedance.

Three varieties of Kevlar[®] were tested: 1) Kevlar 120[®], 7.9 grams/cm² (1.8 oz/in²), "thin weave," 2) Kevlar 124[®], 7.9 grams/cm² (1.8 oz/in²), "crow's foot weave," and 3) Kevlar 500[®], 22.0 grams/cm² (5.0 oz/in²), "thick weave." A comparison of acoustic attenuation is shown in Figure 8 for the three varieties of Kevlar[®]. Because the thick Kevlar[®] cloth showed significant attenuation of source level, it was not used for the wind tunnel tests. In contrast, the thin weave Kevlar[®] showed little acoustic attenuation up to 25 kHz. Both the Recessed Thin Kevlar (RTK), shown in Figure 9, and the Recessed "Crow's Foot" Kevlar (RCFK) were used during the CMT and Array Concept tests. (The horizontal and vertical lines, which appear in the photograph of Figure 9, are artifacts of the stretching of the bi-tropic Kevlar material.)

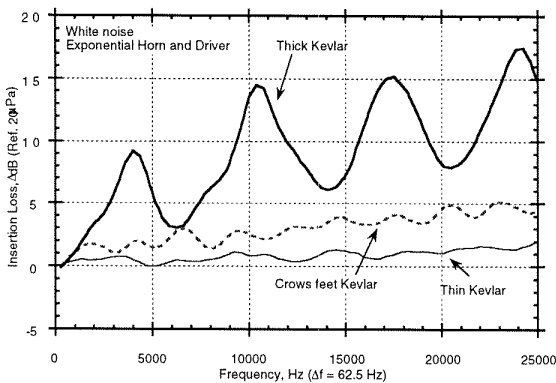


Figure 8. Anechoic chamber test of material insertion loss using a speaker as the source. The thin Kevlar[®] produced the least amount of attenuation.

A comparison of the flush and RTK 70-element array is shown in Figure 10 for a 20.3 cm (8.0 in) wide exponential horn with white noise. The horn was at an oblique angle of -35° to the array centerline. The graph shows the maximum array level for the chosen scan plane. The recessed Kevlar array shows some attenuation, for this case, up to 2.0 dB above 6000 Hz.

Wind Tunnel Test Results

Results from the two wind tunnel investigations revealed a significant reduction in flow-induced background noise attributable to the surface treatment. As suggested by Equation (10), the flow noise should decrease with frequency. For the empty wind tunnel case at Mach 0.22, a comparison of average array microphone sound pressure level is shown in Figure 11 for the flush-mounted and recessed 70-element array microphones. The flow noise at the lower frequencies has been reduced by almost 20 dB. The background noise at high frequency is probably caused by the interaction of the flow and surface sheet. The predicted recessed background noise, based on the wavy wall decay presented in Figure 3, is plotted alongside the two curves. It shows good agreement at low frequencies, as expected.

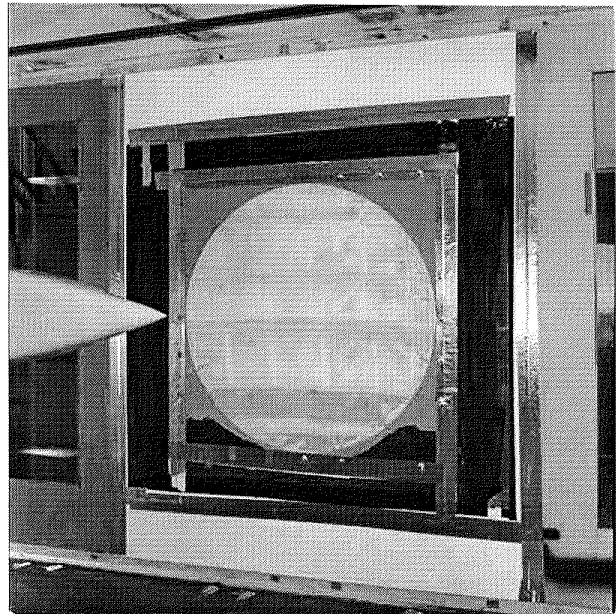


Figure 9. Recessed 70-element array with thin Kevlar[®] screen. The tail of the IMAS is in the foreground.

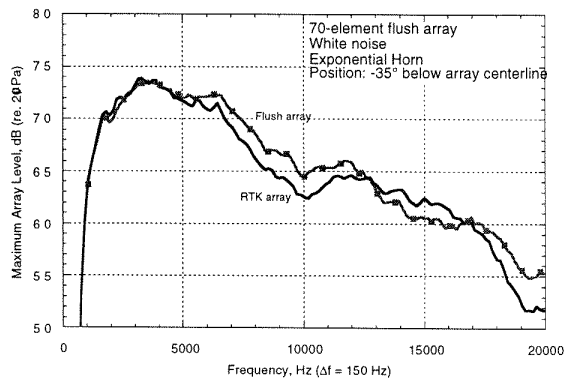


Figure 10. Maximum array level for a 20.3 cm (8.0 in) wide exponential horn, in an anechoic chamber, mounted 2.13 m (84.0 in) away at -35° below the array centerline. Flush-mounted and recessed thin Kevlar, 70-element array.

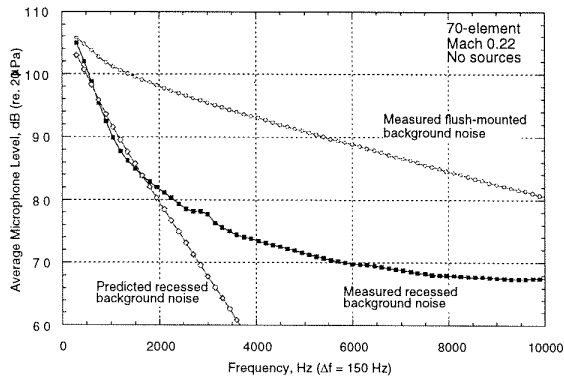


Figure 11. Average microphone sound pressure level in the empty 7x10 wind tunnel for the flush-mounted and RCFK 70-element arrays.

One important aspect of array flow-noise reduction is the dramatic effect on the dynamic range afforded to each microphone. An extra 15 dB in dynamic range is useful when each channel measures, at most, 84 dB. This improvement in dynamic range can be seen by looking at three curves, shown in Figure 12, provided by the processing software for evaluating the array capability: 1) The average microphone sound pressure level, approximately equivalent to what one microphone would measure, 2) the maximum array level at a given frequency for the chosen scan plane, indicating the loudest source seen by the array and 3) the average array level at a given frequency within the chosen scan plane. These curves are generated for each array acquisition. The difference between the maximum array level and the average array level can be interpreted as the ability of the array to locate sources. If the average and maximum levels are the same, it suggests that no significant sources can be visualized within the chosen scan plane. The difference between the average microphone sound pressure level and the maximum and average array levels illustrate the benefit of array processing. During these wind tunnel tests, the average microphone sound pressure level was completely dominated by flow noise, yet the array could still resolve sources well below the background noise level.

Figure 12 shows the three curves for a simple flap at 35° and Mach 0.22 for the 100-element flush-mounted array and the 70-element RCFK array. Also plotted is the integrated level for a broadband source detected at the flap edge. The source can be resolved for most of the recessed array case, but was unresolved for most of the flush array case, with the exception of the highest frequencies. The RCFK array attenuates the source by up to 6 dB at the higher frequencies as presented previously in Figure 8.

Ideally, the surface treatment should have no effect on the maximum or average array levels. Its only influence will be on the noise level seen at each microphone. By applying Equation (4), the SNR for each microphone can be evaluated for the cases shown. For a 95% confidence of achieving 0.5 dB accuracy in peak level, with 70 microphones and 400 averages, the SNR is -13.6 dB. This means the source signal can be as much as 13.6 dB below the background level and will still be detectable within a 95% confidence level. For 100 microphones, the SNR

would be -15.2 dB. The corresponding SNR value is shown for each case in Figure 12. Because of this reduction in flow noise, the signal-to-noise ratio of the array-resolved sources relative to the average array level was increased. This capability allowed for identification of sources that could not be imaged with the flush-mounted arrays without greatly increasing acquisition time.

The improved detection of sources is evident in the comparison of simple flap images in Figure 13. The flap is deflected towards the array at +35°. The images are each displayed with a 6 dB range. Figure 13a is an array image from the flush-mounted 100-element array. The image shows a field of random noise at 3150 Hz. In contrast, the 70-element RCFK array in Figure 13b clearly shows the source on the flap edge. The source would otherwise be buried in background noise. Figure 14 shows a similar comparison for a +35° flap case at 6600 Hz. At even higher frequencies, the recessed array and the flush array have about the same capability for detecting sources, since the recessed array does not reduce the high frequency background noise level.

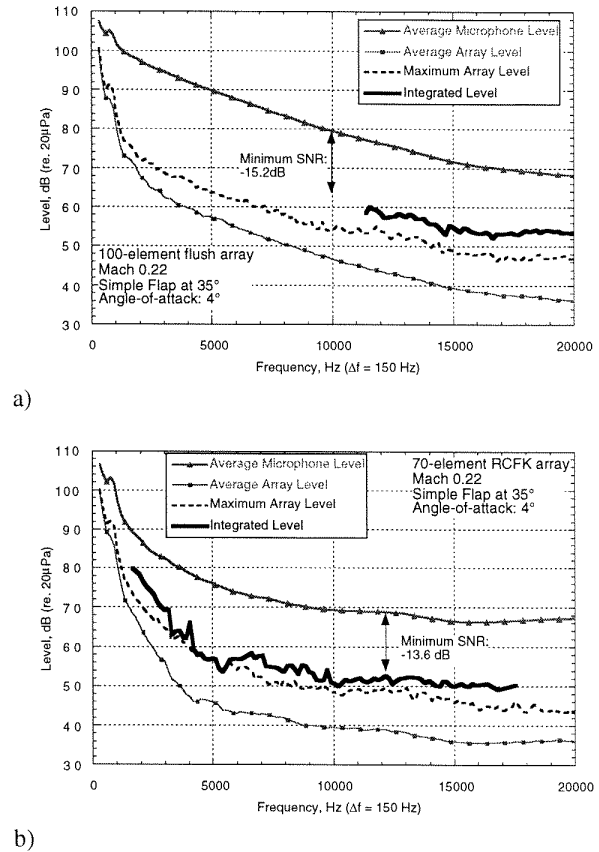
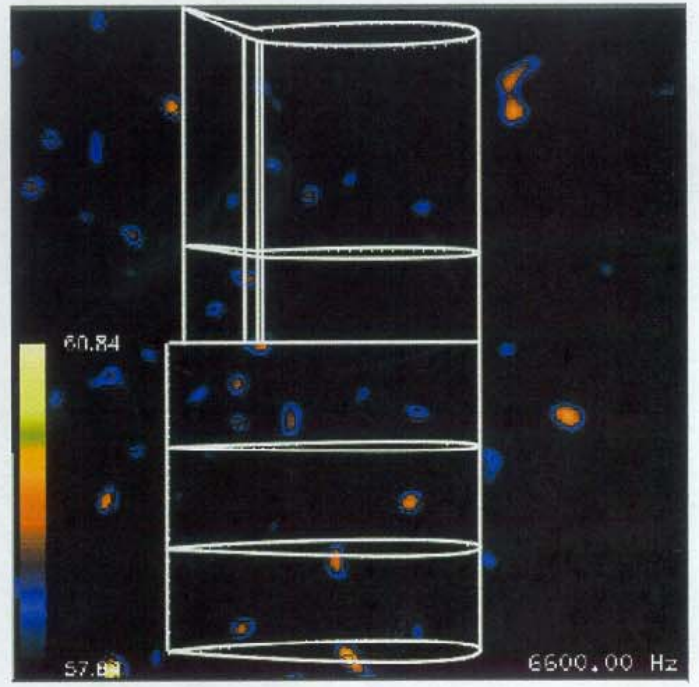


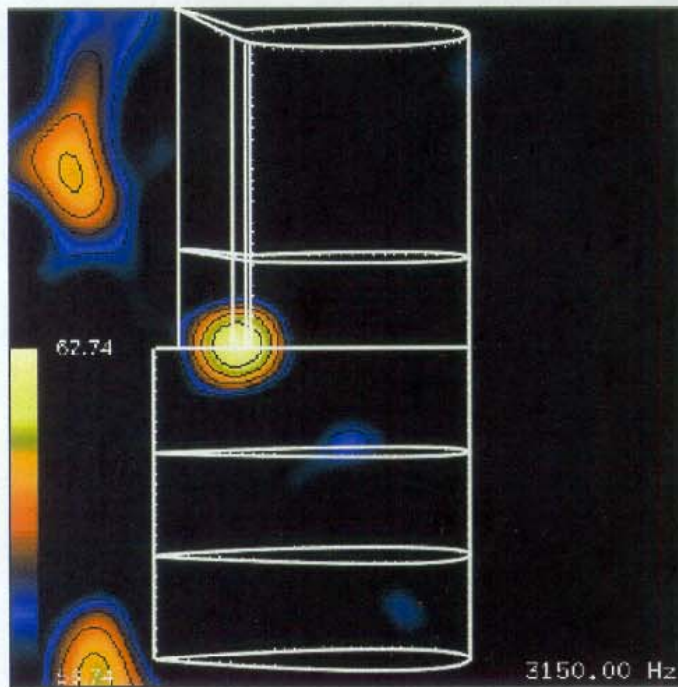
Figure 12. Average microphone level, maximum array level in the scan plane, average array level in the scan plane, and an integrated level for a source. Simple flap at +35°, Mach 0.22 and 4° angle-of-attack. a) 100-element flush-mounted array. b) 70-element RCFK array.



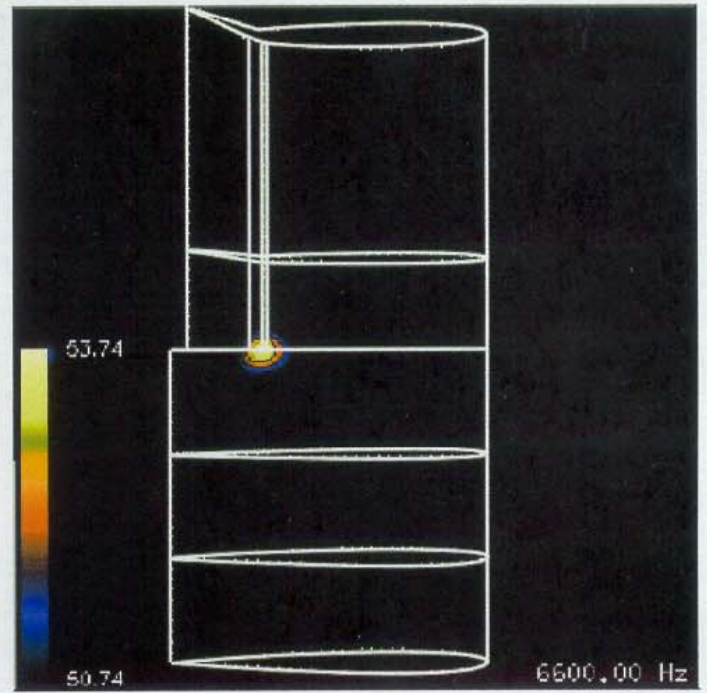
a)



a)



b)

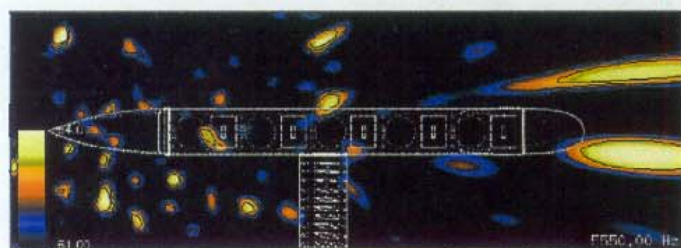


b)

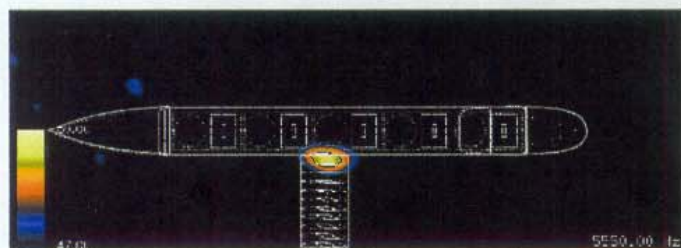
Figure 13. A) Source image for 3150 Hz using flush 100-element array. B) Source image for 3150 Hz using RCFK 70-element array. Simple flap for both cases is set at $+35^\circ$, angle-of-attack of 10° and Mach 0.22.

Figure 14. A) Source image for 6600 Hz using flush 100-element array. B) Source image for 6600 Hz using RCFK 70-element array. Simple flap for both cases is set at $+35^\circ$, angle-of-attack of 4° and Mach 0.22.

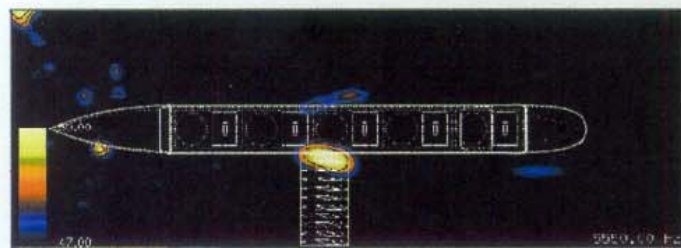
Figure 15 shows the same trend in a comparison of images of the background levels for the IMAS, with speakers turned off, at Mach 0.22. Results at 5500 Hz are shown for the flush mounted 70-element array, the RCFK array and the RTK array. The IMAS was located 1.7 m (67.0 in) from the array. In the cases shown, the array centerline is lined up approximately with the left-most speaker pair. All three images are shown with a 3 dB range, but the average microphone level of the flush mounted array was as much as 15 dB above the average level of the recessed arrays. The flush-mounted array completely overlooks the noise source created at the support junction. Both the RCFK and RTK arrays detect this airframe noise source. At higher frequencies, the recessed array also detected flow disturbances created by bolt heads and other imperfections that were not discernable with the flush array.



a)



b)



c)

Figure 15: Source images for silent IMAS at 5500 Hz and Mach 0.22. A) Flush-mounted 70-element array. B) RCFK 70-element array. C) RTK 70-element array.

CONCLUSION

Careful reduction of flow-induced background noise can greatly increase the utility of microphone arrays for evaluating sources in closed wind tunnels. Although various acquisition and processing techniques exist, there is no good substitute for the reduction of turbulence-generated noise at the microphone diaphragms. The mechanical solution, presented in this paper, provides an acoustically transparent membrane that separates the bare

microphones from the turbulent wind tunnel flow. Specifically, Kevlar® cloth was discovered to be an ideal surface material because of its high shear resistance and low acoustic impedance.

Compared to flush-mounted microphones, the reduction of background noise at frequencies below 3500 Hz was the most dramatic and served to improve the overall dynamic range of the phased microphone array system. This finding implies that the turbulent flow mostly manifests itself as a low frequency background noise, as expected. The surface treatment provides background noise reductions of up to 20 dB. At higher frequencies, the effect is a slight increase in background level, probably as the result of flow interaction with the cloth surface. This paper has demonstrated that investment in even modest flow-induced noise reduction is well warranted when compared with the expense of increasing the number of microphones or increasing wind tunnel test time.

ACKNOWLEDGEMENT

We would like to thank Bruce Storms for his gifted handling of the 7x10 wind tunnel tests and Julie Hayes for her expertise with array image processing.

REFERENCES

1. U. Michel and W. Qiao, "Directivity of Landing-gear Noise Based on Flyover Measurements," 5th AIAA/CEAS Aeroacoustics Conference, Bellevue, WA, AIAA Paper 99-1956, May 10-12, 1999.
2. L. E. Hoglund "The Use of Cross-Correlations in Place of Multiple Sidelines for Source Location," 5th AIAA Aeroacoustics Conference, Seattle, WA, AIAA Paper 79-0618, March 12-14, 1979.
3. R. Sen, "Interpretation of Acoustic Source Maps Made with an Elliptic-Mirror Directional Microphone System," 2nd AIAA/CEAS Aeroacoustics Conference, State College, PA, AIAA Paper 96-1712, May 6-8, 1996.
4. J. M. Kendall Jr., "Airframe Noise Measurements by Acoustic Imaging," 15th AIAA Aerospace Sciences Meeting, Los Angeles, CA, AIAA Paper 77-55, Jan. 1977.
5. S. M. Jaeger and C. S. Allen, "Two-Dimensional Sound Intensity Analysis of Jet Noise," 15th AIAA Aeroacoustics Conference, Long Beach, CA, AIAA Paper 93-4342, Oct. 25-27, 1993.
6. P. T. Soderman and S. C. Noble, "Directional Microphone Array for Acoustic Studies of Wind Tunnel Models," *Journal of Aircraft*, pp. 169-173, 1975.
7. D. Blacodon, M. Caplot, and G. Elias, "A Source Localization Technique for Impulsive Multiple Sources," *Journal of Aircraft*, pp. 154-156, Feb. 1989.
8. T. F. Brooks, M. A. Marcolini, and D. S. Pope, "A Directional Array Approach for the Measurement of Rotor Noise Source Distributions with Controlled

- Spatial Resolution,” *Journal of Sound and Vibration*, Vol. 112, No. 1, pp. 192-197, 1987.
9. G. Elias, “Noise Source Localization with Focussed Antenna for Reduction Purposes” (Transl. from “Localisation par antenne focalisee des sources de bruit en vue de leur reduction”) Science et Defence Conference, Office National d’Etudes et de Recherches Aeronautiques, France, May 1990.
 10. A. H. Pryor, M. Mosher, M. E. Watts, P. Ma, M. B. Reid, and M. J. Barnes, “Noise Level and Location Analysis Report for the High Speed Research Axi-symmetric Mixer Ejector Nozzle (HSR AMEN),” NASA CDTM-21001, January 1995.
 11. M. Mosher, M. E. Watts, M. Barnes, C. S. Allen, S. M. Jaeger, J. A. Hayes, and P. T. Soderman, “Acoustic Array Measurements of 1995 High-Lift Engine Aeroacoustic Technology Test in Ames 40- by 80-Foot Wind Tunnel,” NASA CDTM-21007, June 1996.
 12. P. Sijtsma and H. Holthusen, “Source Location by Phased Array Measurements in Closed Wind Tunnel Test Sections,” 5th AIAA/CEAS Aeroacoustics Conference, Bellevue, WA, AIAA Paper 99-1814, May 10-12, 1999.
 13. T. F. Brooks and W. M. Humphreys, Jr., “Effect of Directional Array Size on the Measurement of Airframe Noise Components,” 5th AIAA/CEAS Aeroacoustics Conference, Bellevue, WA, AIAA Paper 99-1958, May 10-12, 1999.
 14. R. Stoker, “Full-Scale Landing Gear Noise Test Results,” 3rd AST Airframe Noise Workshop, Seattle, WA, Nov. 17-18, 1998
 15. R. P. Dougherty, “Phased Array Beamforming for Aeroacoustics,” AIAA Professional Development Short Course, Bellevue, WA, May 8-9, 1999.
 16. W. C. Horne and K. D. James, “Concepts for Reducing the Self-noise of In-flow Acoustic Sensors and Arrays,” 5th AIAA/CEAS Aeroacoustics Conference, Bellevue, WA, AIAA Paper 99-1815, May 10-12, 1999.
 17. C. S. Allen, K. Vandra, and P. T. Soderman, “Microphone Corrections for Accurate In-Flow Acoustic Measurements at High Frequency,” 1st Joint CEAS/AIAA Aeroacoustics Conference, Munich, Germany, CEAS/AIAA Paper 95-150, June 12-15, 1995.
 18. F. Schmitz, S. Liu, S. M. Jaeger, and W. C. Horne, “Noise Reducing Screens for In-Flow Pressure Sensors,” U. S. Patent No. 5,684,756, Nov. 1997.
 19. S. M. Jaeger, C. S. Allen, and P. T. Soderman, “Reduction of Background Noise in the NASA Ames 40- by 80-Foot Wind Tunnel,” 1st Joint CEAS/AIAA Aeroacoustics Conference, Munich, Germany, CEAS/AIAA Paper 95-152, June 12-15, 1995.
 20. H. U. Hamid and W. C. Horne, “An Experimental Study of the Response of a Condenser Microphone Installed in a Flat Plate,” 35th AIAA Aerospace Sciences Meeting, Reno, NV, AIAA 97-0491, Jan. 6-10, 1997.
 21. H. Liepman and A. Roshko, *Elements of Gas Dynamics*, Wiley and Sons, 1957.
 22. J. R. Underbrink, “Practical Considerations in Focused Array Design for Passive Broadband Source Mapping Applications,” Master’s Thesis, Pennsylvania State University, May 1995.
 23. M. B. Reid, “Design of Optimized Arrays Using Simulated Annealing,” Internal NASA Ames Research Center Document.
 24. C. P. Robert and G. Casella, *Monte Carlo Statistical Methods*, Springer-Verlag, pp.199-201, 1999
 25. R. Rew, G. Davis, S. Emmerson, and H. Davies, *Net CDF User’s Guide for C*, University Corporation for Atmospheric Research, Boulder, CO, June 1997. www.unidata.ucar.edu/packages/netcdf/.
 26. M. E. Watts, M. Mosher, and M. J. Barnes, “The Microphone Array Phased Processing System (MAPPS),” 2nd AIAA/CEAS Aeroacoustics Conference, State College, PA, AIAA Paper 96-1714, May 6-8, 1996.
 27. M. Mosher, “Phased Arrays for Aeroacoustic Testing: Theoretical Development,” 2nd AIAA/CEAS Aeroacoustics Conference, State College, PA, AIAA Paper 96-1713, May 6-8, 1996.
 28. B. L. Storms, J. A. Hayes, S. M. Jaeger, and P. T. Soderman, “Aeroacoustic Study of Flap-tip Noise Reduction Using Continuous Moldline Technology,” 6th AIAA/CEAS Aeroacoustics Conference, Lahaina, HI, AIAA 2000-1976, June 2000.
 29. M. W. Geiger and J. C. Waldrop, “Continuous Moldline Technology System,” U.S. Patent No. 5,810,291, Sept. 1998.
 30. W. C. Horne, S. M. Jaeger, J. A. Hayes, and S. Jovic, “Effects of Distributed Source Coherence on the Response of Acoustic Arrays,” 6th AIAA/CEAS Aeroacoustics Conference, Lahaina, HI, AIAA 2000-1935, June 2000.
 31. *Mark’s Standard Handbook for Mechanical Engineers*, 10th ed., McGraw-Hill, Ch.11-112, 1996.